CVGIP: GRAPHICAL MODELS AND IMAGE PROCESSING
Vol. 53, No. 5, September, pp. 403–412, 1991

Robust Identification of Motion and Out-of-Focus Blur Parameters from Blurred and Noisy Images

R. FABIAN* AND D. MALAH

Department of Electrical Engineering, Technion—Israel Institute of Technology, Haifa 32000, Israel

Received July 29, 1988, accepted November 28, 1990

Most image deblurring methods assume knowledge of the point spread function (PSF) causing the blur. In this work we address the problem of identifying the characterizing parameter of the PSF, which corresponds to motion or out-of-focus blur, from blurred and noisy images. The observation that the spectra of these blurring functions have periodic (or almost periodic) zeros is the basis of an already known blur identification method in the cepstral domain. However, this method is found to be highly sensitive to noise. In this paper we propose the following improvements on the above method: First, adding a preprocessing stage for noise reduction, using a modified spectral subtraction approach—with a median-complement filter to estimate the noise. Second, applying an adaptive, quefrency-varying, comb-like window (lifter) in the cepstral domain to enhance the blur parameter identification. The robustness of the proposed algorithm is demonstrated by its ability to identify the blur function parameters from noisy blurred images with signal-to-noise ratio down to 0 dB for motion blur and 3 dB for out-of-focus blur, as compared to 20 dB for the original method.

1. INTRODUCTION

The problem of restoring noisy images has been a difficult challenge for many years and is addressed in numerous publications. The main trends and methods in restoration can be found in several books, such as [1, 21–25], and in a recent survey paper [26].

The majority of image restoration algorithms require some knowledge about the degradation process and associated parameters. These include the classical Wiener filter restoration techniques [1, 21–25], the more recent iterative restoration algorithms [15, 16, 26, 27], and others [17–19, 26]. The problem is that the information required is not always available and that the restoration results were found to be highly dependent on the blurring-system model used and on the accuracy by which its parameters are identified from the degraded image. The approaches taken in many image restoration works for overcoming the problem can be put into one of the following two categories:

a. Identification of the point spread function (PSF) parameters in order to use them later in one of the known restoration algorithms.

b. Incorporation of the identification procedure into the restoration algorithm.

The work of Gennery [2], who tried to identify the PSF parameters in the spectral domain, the work of Mitre and Fleuret [7], on identification in both the spatial and the spectral domains, and the works by Cole [6] and Cannon [3–5], on identification in the log-spectral and cepstral domains, all fall in the first category. The works of Biemond and Van der Putten [12] and Tekalp and Kaufman [10, 11] can be considered as members of the second category. The principal attitude in [10–12] is to assume that the degraded image can be modeled as a product of an ARMA system, where the autoregressive part represents the image, and the moving average part represents the degradation process.

Cooke and Dorrani [8, 9] assume a new model for the degraded image formation and propose an iterative process for combined identification and restoration, and thus also belong to the second category. The main drawback of all the above-mentioned methods is the high sensitivity to additive noise. The relatively simple methods of [2] and [7] are restricted to very high signal-to-noise ratios (SNR) of the degraded image under test. In papers [6, 8–10, 12], the lowest SNR reported is 20 dB. This was also the result in our examination of Cannon's method [4].

In this paper we present a robust method for identifying the PSF parameters from motion and out-of-focus blurred images with additive noise, which is partly based on the approach in [4].

Section 2 of this paper presents the blurring-system model used and its representation in the spatial, spectral, and cepstral domains. Cannon's algorithm is described in Section 3. The spectral subtraction approach and its implementation are the subject of Section 4. Section 5 gives a detailed description of the proposed algorithm and in

* Presently with RAFAEL—Armament Development Authority, Haifa, Israel.

1049-9652/91 $3.00

Section 6 simulation results are presented. Section 7 provides a summary and conclusions.

2. BLURRING-SYSTEM MODEL

We assume that the image acquisition process is as depicted in Fig. 1 with a linear space-invariant imaging system.

Mathematically, it can be described as

$$g(x, y) = f(x, y) * h(x, y) + n(x, y), \tag{1}$$

where $f(x, y)$ is the original image; $g(x, y)$, the observed image; $h(x, y)$, the point spread function of the imaging system; $n(x, y)$, additive noise; and $*$, the convolution operator.

In the Fourier transform domain, Eq. (1) takes the form

$$G(u, v) = F(u, v) \cdot H(u, v) + N(u, v). \tag{2}$$

2.1. *Blur Functions*

As noted above, two types of blur functions are dealt with in this paper: motion blur, caused by relative motion between the object and the camera along the x axis during exposure time, and out-of-focus blur, caused by the camera's lens, having a circular aperture, being defocused.

For motion blur, $h(x, y)$ is given by the one-dimensional rectangle

$$h(x, y) = \begin{cases} 1/d, & -d/2 \le x \le d/2;\ y = 0, \\ 0, & \text{otherwise}, \end{cases} \tag{3}$$

where d is the "blur length" and is proportional to the relative velocity between the camera and the object and to the film exposure time. The Fourier transform of $h(x, y)$ in this case is

$$H(u, v) = \frac{\sin(\pi du)}{\pi du} = \operatorname{sinc}(\pi du). \tag{4}$$

The amplitude of $H(u, v)$ is characterized by periodic zeros on the u axis, which occur at

$$u = \pm \frac{1}{d}, \pm \frac{2}{d}, \pm \frac{3}{d}, \cdots. \tag{5}$$

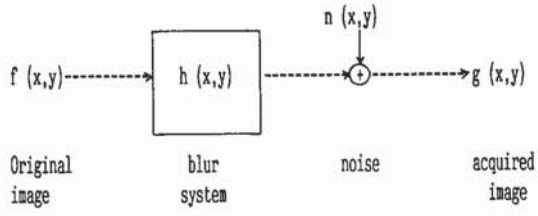

FIG. 1. Image acquisition process.

For out-of-focus blur, $h(x, y)$ is assumed to be given by the cylinder

$$h(x, y) = \begin{cases} 1/\pi R^2, & x^2 + y^2 \le R^2, \\ 0, & \text{otherwise}, \end{cases} \tag{6}$$

where R is the "blur radius" and is proportional to the extent of defocusing. The Fourier transform of $h(x, y)$ in this case is

$$H(u, v) = J_1(\pi Rr)/\pi Rr, \tag{7}$$

where $r^2 = u^2 + v^2$ and $J_1(\cdot)$ is the first-order Bessel function of the first kind. The amplitude of $H(u, v)$ is characterized by "almost-periodic" circles of radius r, at which $H(u, v)$ takes the value zero. This occurs at values of r satisfying

$$2\pi Rr = 3.83,\ 7.02,\ 10.2\ 13.3,\ 16.5, \cdots. \tag{8}$$

It is seen therefore that these two types of blurs are each characterized by a PSF which requires only a single parameter for its complete determination.

2.2. *Cepstral Representation*

The cepstral representation of the blur function $h(x, y)$ is given by

$$C_h(p, q) = F^{-1}\{\log|H(u, v)|\}, \tag{9}$$

where F^{-1} denotes the inverse Fourier transform. Note that since $|(H(u, v)|$ is real and even, so is $C_h(p, q)$.

For motion blur, it is recalled that the distance between adjacent zeros of the blur function spectrum is $1/d$. Representing this function in the cepstral domain results in a distinct negative pulse at a distance d from the origin and replicas of this pulse at integer multiples of d.

For out-of-focus blur, $H(u, v)$ has almost-periodic circles of zero value where the distances between adjacent circles is approximately $1/(2R)$. Representation of the blur function in the cepstral domain gives a distinct circle of negative amplitude with a radius of approximately $2R$ and "replicas" of this circle with radii which are approximately multiples of $2R$.

3. CANNON'S APPROACH

In his works [3–5], Cannon found out that the noise added to the blurred image is the main cause for the "disappearance" of zeros of the PSF in the spectral do-

main and therefore prevents their identification in the cepstral domain. He proposed therefore the following scheme: The assumption that the image and the noise are samples of a stationary random process gives, from (2),

$$P_g(u, v) = P_f(u, v) \cdot |H(u, v)|^2 + P_n(u, v), \quad (10)$$

where $P_g(u, v)$, $P_f(u, v)$, and $P_n(u, v)$ denote the power spectra of $g(x, y)$, $f(x, y)$, and $n(x, y)$, respectively.

An estimate of $P_g(u, v)$ can be obtained using Welch's algorithm [14]. This is done by dividing the image into subimages, multiplying each subimage by a 2D Hamming window, computing its squared magnitude Fourier transform (modified periodogram), and averaging over all subimages, resulting in

$$\hat{P}_g(u, v) = \overline{P_f(u, v)} \cdot |H(u, v)|^2 + \overline{P_n(u, v)}, \quad (11)$$

Assuming that the noise is white, $\overline{P_n(u, v)}$ converges (as the number of subimages grows) to a constant which equals to the noise variance. It is evident that if the noise variance is sufficiently small, conspicuous negative peaks in the cepstral domain can be expected at locations which are multiples of the blur parameters, as explained above, and they will dominate the form of $C_{\hat{g}}(p, q)$—the cepstral representation of $P_{\hat{g}}(u, v) \triangleq \hat{P}_g(u, v)$. Identification can thus be achieved by a careful examination of $C_{\hat{g}}(p, q)$.

As was mentioned earlier, the main drawback of this algorithm is its high sensitivity to additive noise. The main goal of this paper is therefore to modify the above approach and make it more robust to high-level noise. The first step in our proposed algorithm is noise reduction by spectral subtraction, as elaborated next.

4. NOISE REDUCTION BY SPECTRAL SUBTRACTION

In comparing several methods, we found that the spectral subtraction method, when applied to the *whole image* (without subdivision of the image, as is more common for image enhancement [13]), is most effective as a preprocessing operation for noise reduction when the aim is to identify the blur function parameter in the cepstral domain.

A detailed development and description of the spectral subtraction algorithm is given in [13]. Here we briefly present the main result: Let $b(x, y)$ denote the blurred only (noise-free) image. Hence, Eq. (1) takes the form

$$g(x, y) = b(x, y) + n(x, y). \quad (12)$$

Estimation of the Fourier transform of $b(x, y)$, $B(u, v)$, from the Fourier transform of $g(x, y)$, $G(u, v)$, using the power spectrum method [1], results in the following formulation of the spectral subtraction algorithm [13],

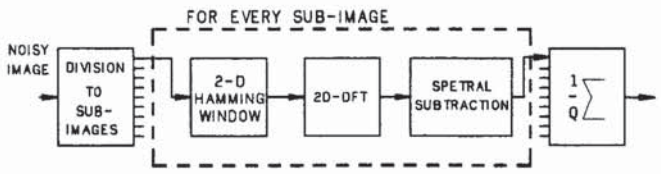

FIG. 2. Integration of the spectral subtraction algorithm into Cannon's approach.

$$\begin{aligned} |\hat{B}(u, v)| &= [|G(u, v)|^2 - \alpha \cdot P_n(u, v)]^{1/2} \\ &\qquad \text{if } |G(u, v)|^2 > \alpha \cdot P_n(u, v) \\ |\hat{B}(u, v)| &= \varepsilon \qquad \text{otherwise} \\ \measuredangle \hat{B}(u, v) &= \measuredangle G(u, v), \end{aligned} \quad (13)$$

where α is a coefficient used to control the subtraction extent and ε is a small constant used to avoid numerical difficulties when one is taking the logarithm of $|\hat{B}(u, v)|$.

A method for estimating $P_n(u, v)$ is explained in Section 5. Note that in our application no use is made of the phase $\measuredangle \hat{B}(u, v)$), as no reconstruction of the enhanced image is sought here.

Because of image nonstationarity, it is common to apply the spectral subtraction technique to subimages of the given image and then recombine the enhanced subimages to obtain the restored image. It appears therefore that combining this enhancement technique with the spectral averaging of subimages used in Cannon's algorithm can be done quite efficiently as depicted in Fig. 2.

However, the performance of this approach, *in the context of blur parameter identification,* using both our algorithm (Section 5.2) and Canon's algorithm, was found to be lower than if the spectral subtraction method method is applied to the *whole* image, as described in Section 5.1.

It should be emphasized again that since the goal here is *not* the restoration of the image but rather the extraction of the blur function parameter, our judgment of the noise reduction technique applied is based only on the ability to identify the blur parameters and not on the enhancement of the image. Once the parameter is found, any desired enhancement and restoration techniques can be applied.

5. ALGORITHM DESCRIPTION

The proposed algorithm has two stages. In the first stage a form of the spectral subtraction method is employed for noise reduction. In the second stage the enhanced spectral magnitude function is transformed to the cepstral domain and the identification procedure is completed using an adaptive, quefrency-varying, "comb-like" window (lifter).[1]

[1] The notions of "quefrency" and "lifter" are commonly used in cepstral domain processing [29].

5.1. *Stage I: Noise Reduction*

The noise reduction procedure in this stage follows the spectral subtraction formulation given in (13), with $\varepsilon = 1 \cdot E - 10$ and $\alpha = 1$, but is applied to the whole image, without dividing it into subimages as discussed above.

The selection of $\alpha = 1$ is based on testing the proposed approach on three test images using several values for α in the range of (0.1 to 1.0). This result could have been expected in view of the fact that a higher value of α "uncovers" more zeros in the spectral domain, with the desired ones, due to the PSF, being enhanced by the comb lifter in the cepstral domain, as explained in Section 5.2.

It remains to obtain a good estimate of $P_n(u, v)$: On the basis of our previous experience with median filters and on the basis of published results on its performance for noise suppression (e.g., see [28]), we used a median filter to generate a "median-complement" image, defined below, in order to obtain an estimate of the noise, $\hat{n}(x, y)$, from which an estimate of $P_n(u, v)$ is computed.

A median filter [1] is defined as follows: Let $\{a_n\}_{n=1}^{2K+1}$ be an input sequence of length $2K + 1$. $\{a_n\}$ is reordered to get the sequence $\{b_n\}_{n=1}^{2K+1}$, according to the law

$$b_{n_2} \geq b_{n_1} \leftrightarrow n_2 > n_1; \tag{14}$$

then

$$\text{Median } \{a_n\}_{n=1}^{2K+1} \triangleq b_{K+1}, \tag{15}$$

i.e., the median is given by the center element of the rank (amplitude) ordered sequence $\{b_n\}$. A median-complement filter is thus defined by

$$\text{Median-Complement } \{a_n\}_1^{2K+1} \triangleq a_{K+1} - b_{K+1}. \tag{16}$$

Applying this procedure to the problem at hand results in

$$\hat{n}(x, y) = \text{Median-Complement } \{g(x, y)\} \tag{17}$$

and we let

$$\hat{P}_n(u, v) = P_{\hat{n}}(u, v) \triangleq |\hat{N}(u, v)|^2, \tag{18}$$

where $\hat{N}(u, v)$ is the Fourier transform of $\hat{n}(x, y)$. On the basis of an examination of several filter lengths and types (1D and 2D), and because blurred images are rather smooth, we found that the simplest median filter, 1D of length 3 (i.e., $K = 1$), is suitable for the above task.

The block diagram of this stage appears in Fig. 3. In the upper path the noise is estimated from the original image by a median-complement filter, as explained above. The output of this filter is multiplied by a 2D Hamming window prior to the Fourier transformation.

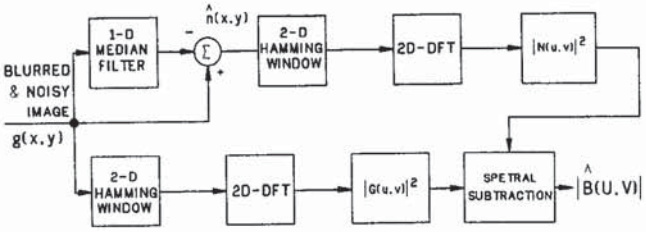

FIG. 3. Block diagram of Stage I in the proposed algorithm.

In the lower path the power spectrum of the input (blurred and noisy) image is estimated from the 2D Hamming windowed and Fourier transformed image. The resulting periodograms $|G(u, v)|^2$ and $\hat{N}(u, v)|^2$ enter the spectral subtraction unit, giving $|\hat{B}(u, v)|$.

5.2. *Stage II: Blur Parameter Identification*

We have seen already that the cepstral representation of the PSF is dominating the form of the cepstral representation of the blurred image. Therefore, the same domination is expected in $C_{\hat{b}}(p, q)$—the cepstral representation of the enhanced (using spectral subtraction) blurred image. For motion blur, a distinct negative pulse is expected on the p axis, whereas for out-of-focus blur, a distinct circle of negative values is expected.

Although it seems sufficient to examine the one-dimensional sequence $C_{\hat{b}}(p, 0)$ and look for a negative dominant pulse, in the presence of noise this was found to be effective only for the motion blur case. For out-of-focus blur the following approach is taken: First, $C_{\hat{b}}(p, q)$ is converted to a polar coordinate representation to get $C_{\hat{b}}(r, \theta)$. Then, the sequence $C_{\hat{b}}(r)$ is created by averaging over θ:

$$C_{\hat{b}}(r) = \frac{1}{2\pi} \int_0^{2\pi} C_{\hat{b}}(r, \theta)\, d\theta. \tag{19}$$

Thus, all the information available along a circle of some radius r_0 in $C_{\hat{b}}(p, q)$ is concentrated at the single point $C_{\hat{b}}(r_0)$.

Since a one-dimensional sequence is eventually used for identifying the blur parameter in both cases, we examined ways to reduce the amount of computation. For the motion blur case this is quite simple, since by the "projection-slice" theorem [20],

$$C_{\hat{b}}(p, 0) = F^{-1}\{s(u)\}, \tag{20}$$

where

$$s(u) = \int_{-\infty}^{\infty} \log|B(u, v)|^2\, dv; \tag{21}$$

i.e., $C_{\hat{b}}(p, 0)$ can be obtained from the inverse 1D Fourier transform of the 1D sequence obtained by averaging $\log|B(u, v)|^2$ along the columns (following, of course, discretization of the (u, v) frequency axes).

For the out-of-focus case, an attempt to apply a similar theorem in polar coordinates (to obtain $C_{\hat{b}}(r)$) did not lead to the sought simplification since a Hankel transform, which is not simple to compute, is involved. Thus, in this case, a 2D Fourier transform is applied to obtain $C_{\hat{b}}(p, q)$, which is then converted to polar coordinates and averaged along circles to obtain the 1D sequence $C_{\hat{b}}(r)$. The conversion to polar coordinates is done on a discrete polar grid for which the radii get integer values in the range (0, 255) and the angles (in degrees) get integer values in the range (0, 359). To simplify the conversion, each point on the discrete polar grid is assigned the value given to its "nearest neighbor" on the Cartesian grid.

For convenience of the pursuing development we denote the 1D sequence obtained in each of the two cases by $C_{\hat{b}}(m)$ (or, if no spectral subtraction is applied, by $C_g(m)$).

We mentioned before that the desired negative pulse in the examined cepstral sequence is accompanied by its replicas and other pulses which result from the additive noise and the original image itself. At low noise levels these pulses are usually of lower amplitudes than the desired first pulse. However, at higher noise levels (e.g., SNR values below 10 dB), this is not the case and misidentification occurs.

To overcome the problem we propose the following algorithm, which aims to suppress undesired negative pulses and enhance the desired one. According to this algorithm the cepstral sequence $C_{\hat{b}}(m)$ is modified into a new sequence $C(m)$ as shown in Eq. (22), below. This is done by dividing the absolute value of each point in $C_{\hat{b}}(m)$, for which $C_{\hat{b}}(m)$ is negative, by the RMS value of all the negative terms ("pulses") that can be considered as *disturbing* pulses with respect to this point. An adaptive, quefrency-varying (i.e., dependent on the index of the examined point), comb-like window (lifter) is used to omit points at multiples of the index of the examined point since these points are not considered disturbing pulses. The pass and stop bands of the lifter are matched to each examined point in the sequence and therefore are at different locations for different examined points, as illustrated in Fig. 4. This figure is further discussed in the sequel. It can be seen from (22) that the lifter actually scans the sequence $C_{\hat{b}}(m)$ and a "signal-to-disturbance" ratio at each point, for which $C_{\hat{b}}(m) < 0$, is computed. The scanning is done for values of m in the range $m_0 < m < N/2$, where $m_0 \geq 0$, and N is the size of the discrete Fourier transform (DFT). If some a priori knowledge on the range of the blur extent is available, m_0 can be set just below the lowest end of this range (in pixels).

The mathematical formulation for computing the modified sequence $C(m)$ is given by

$$C(m) = \begin{cases} 0 & \text{if } C_{\hat{b}}(m) \geq 0, \\ |C_{\hat{b}}(m)| \Big/ \left[\dfrac{1}{M_m} \displaystyle\sum_{l \in A_m} (C_{\hat{b}}(l))^2\right]^{1/2} & \text{if } C_{\hat{b}}(m) < 0, \end{cases} \tag{22}$$

where

m the examined point index, $m_0 < m < N/2$;
A_m the "disturbance set," corresponding to point m, which contains the indices of all the points in $C_{\hat{b}}(\cdot)$ having a negative value, and:
—have an index greater than m_0
—do not coincide with the examined point
—do not have an index which is ± 1 of an integer multiple of m;
M_m total number of points in A_m.

Note that if for some examined point $m = m_z$, $C_{\hat{b}}(m_z) < 0$ and A_m is empty (i.e., $M_m = 0$), one should set

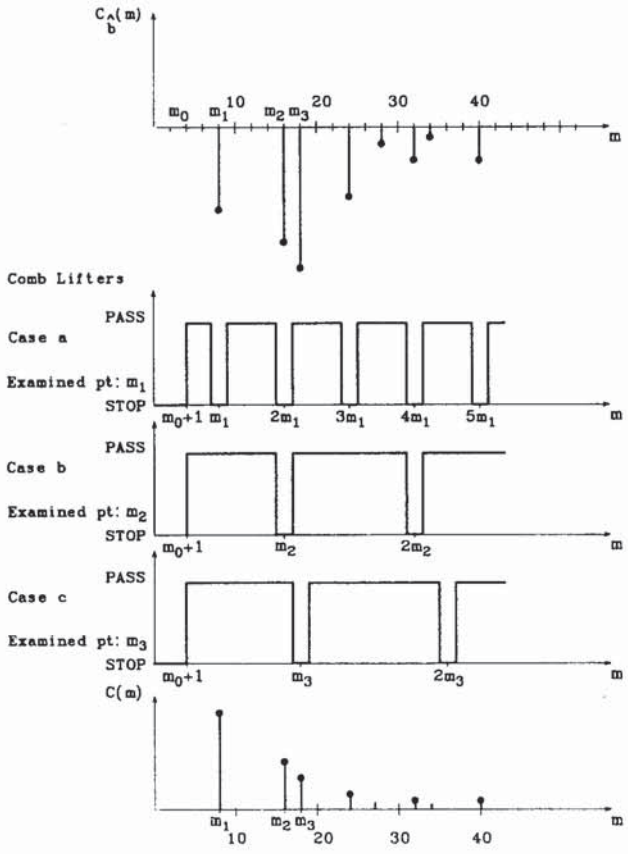

FIG. 4. Graphic demonstration of the application of the comb lifter to generate the modified cepstral sequence $C(m)$.

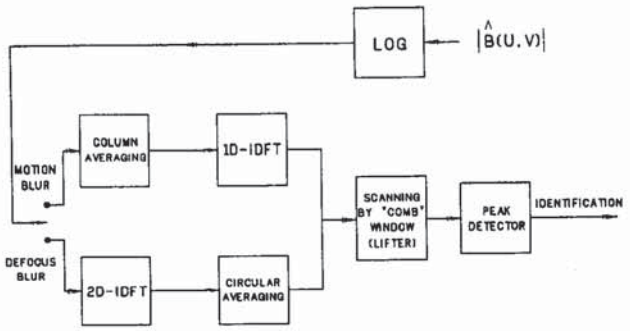

FIG. 5. Block diagram of Stage II in the proposed algorithm.

$C(m_z) = |C_{\hat{b}}(m_z)|$. Such a situation may occur for values of m in the range $m_0 \leq m \leq 3$, if m_0 is set in the range $0 \leq m_0 \leq 2$, because the stop band of the comb lifter is 3 points wide (± 1 about the center point). Thus, if $m_0 \geq 3$ is used (assuming that the blur extent is more than 3 pixels) the situation of obtaining an empty A_m is usually avoided. The reason for using a 3-point stop band is to allow for discretization errors and for the fact that the spectral zeros obtained with out-of-focus blur are not exactly periodic.

The terms in the resulting sequence $C(m)$ are all positive and thus identification can be achieved by activating a peak detector on this sequence.

The following three cases, which are demonstrated in Fig. 4, are of interest:

a. m is the index of the desired pulse (in Fig. 4, $m = m_1$): In this case, pulses at integer multiples of m are not included in A_m. Thus, A_m contains only the indices of "noise points" and $C(m)$ will typically get a high positive value.

b. m coincides with the index of a replica of the desired pulse (e.g., in Fig. 4, $m = m_2 = 2m_1$): In this case, A_m contains the indices of the desired pulse, some of its replicas, and some noise points. Hence, $C(m)$ gets a low value (relative to Case a).

c. m is some point that does not fit the description in the former two cases (e.g., in Fig. 4, $m = m_3$): In this case, A_m consists of the indices of the desired pulse, most of its replicas, and some noise points. Thus, $C(m)$ will get even a lower value than in Case b.

A block diagram of this stage (Stage II) appears in Fig. 5. A different processing path is taken for each of the blur types under consideration in order to generate $C_{\hat{b}}(m)$, as explained above. The adaptive comb lifter is then applied to this sequence to create the modified sequence $C(m)$ according to (22).

6. RESULTS

Experiments were conducted in which pictures were synthetically degraded by a computer so that the extent of the blur and the amount of noise corruption could be completely controllable. This way the robustness of the algorithm to noise could be measured by determining the lowest value of the input signal-to-noise ratio for which the correct blur parameter is still obtained.

The algorithm was tested for the two blur types and various values of the blur parameters. For motion blur, the blur length d was given values of 8, 11, and 19 pixels. For out-of-focus blur, the blur radius R was given values of 8 and 12 pixels.

The signal-to-noise ratio is defined here as:

$$SNR = 10 \log \left\{ \frac{\text{variance of signal}}{\text{variance of noise}} \right\}. \tag{23}$$

Examples of results obtained in the experiments appear in Table 1.

It is seen from the table that the performance for the out-of-focus blur is somewhat lower than that for motion blur. This can be attributed to the fact that the spectral zeros due to the PSF are not exactly periodic for out-of-focus blur and to the errors involved in converting from Cartesian to polar coordinates on a discrete grid using the simple interpolation method (nearest neighbor) described above.

Examples of images and signals in the spatial, spectral, and cepstral domains are shown in the following figures. One of the original test images appears in Fig. 6. Its motion blurred (with $d = 19$) and out-of-focus blurred (with $R = 8$) versions appear in Fig. 7 and Fig. 8, respectively. The representations of these two images in the spectral domain appear in Fig. 9 and Fig. 10, respectively, in which the lines and circles at which the amplitude is zero are clearly seen. The negative terms of the cepstral domain representation of the defocused blurred image are shown as white points in Fig. 11. Again, a distinct circle of a very high negative amplitude is clearly seen. These phenomena, in the spectral and cepstral domains, actually disappear when noise is added to the blurred images, as exemplified in Fig. 12. Therefore, it is much more

TABLE 1
Minimum Input SNR Required for Blur Parameter Identification

	Blur type and extent			
	Motion $d = 11$	Motion $d = 19$	Defocus $R = 8$	Defocus $R = 12$
SNR (dB) →	0.7	−0.4	3.1	2.8

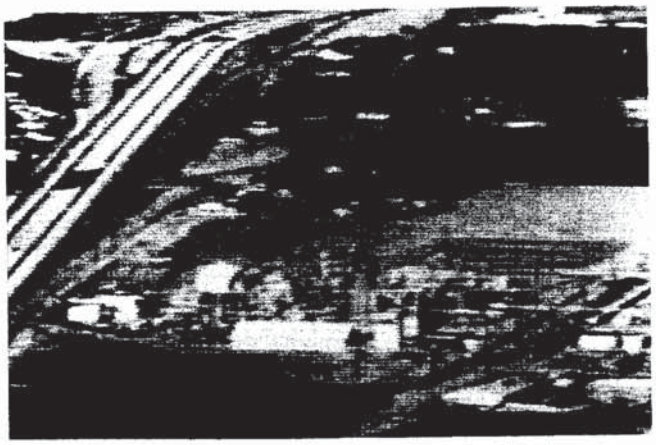

FIG. 6. Original test image (256 × 256 × 8 bits).

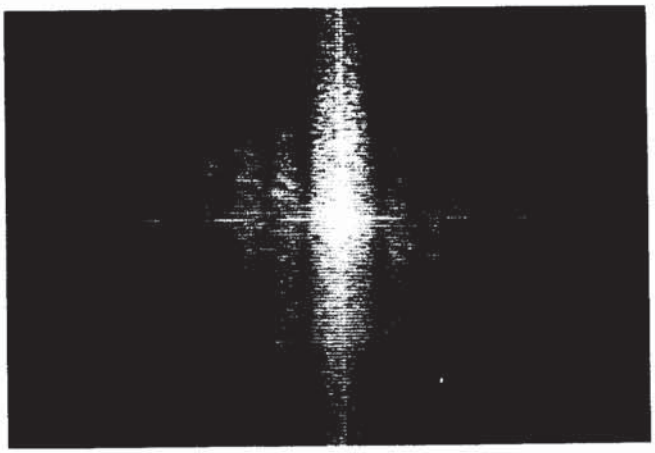

FIG. 9. Spectral representation of the image in Fig. 7.

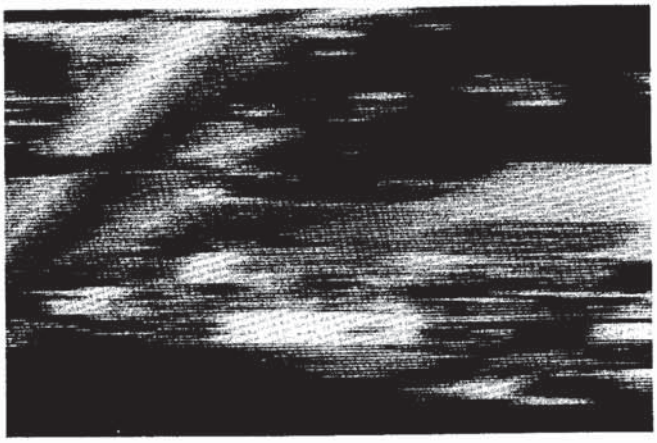

FIG. 7. Motion blurred version (d = 19) of test image.

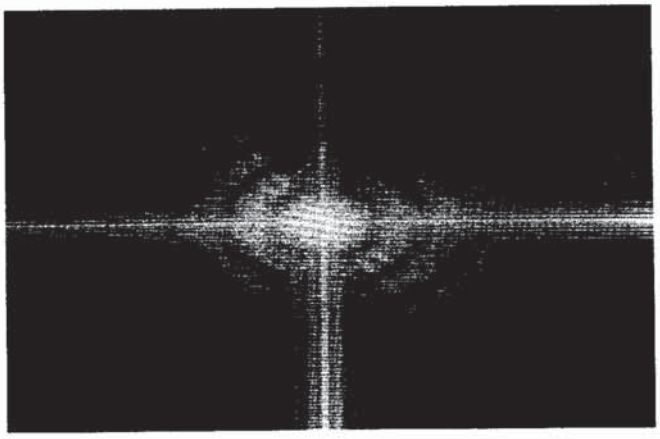

FIG. 10. Spectral representation of the image in Fig. 8.

FIG. 8. Defocus blurred version (R = 8) of test image.

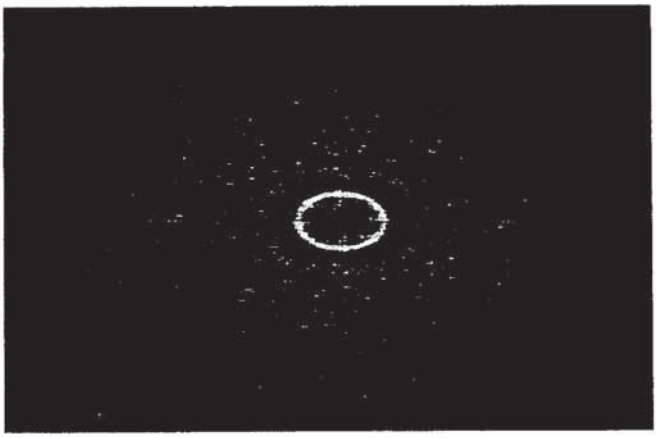

FIG. 11. Negative terms of the cepstral representation of the image in Fig. 8.

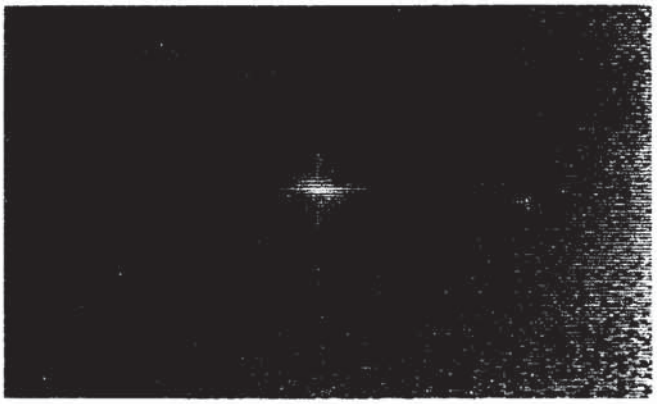

FIG. 12. Spectral representation of defocus blurred (R = 8) and noisy (SNR = 3 dB) test image.

meaningful to demonstrate the various steps of the algorithm using 1D output sequences as shown in the following figures.

Figure 13 shows the negative terms of $C_g(p, 0)$ for the noise-free motion blurred test image. Figure 14 shows the negative terms of $C_g(p, 0)$ for an SNR of 0 dB. One can see that the distinct pulse that appeared in Fig. 13 is no longer conspicuous. When the spectral subtraction algorithm is applied to the distorted image, the desired pulse in the cepstral domain sequence $C_{\hat{b}}(p, 0)$ gets a much higher value but it still cannot be detected by simple means, as evident from Figure 15. Figure 16 shows the cepstral sequence $C(m)$ which results from applying the comb lifter to $C_{\hat{b}}(m)$ according to (22). It can easily be seen that the desired pulse is now detectable by means of a peak detector and hence correct identification is accomplished.

Figures 17 to 19 are like Figs. 14 to 16, but for out-of-focus blur with R = 8 and an input SNR of 3 dB. These figures too demonstrate the effectiveness of the proposed algorithm.

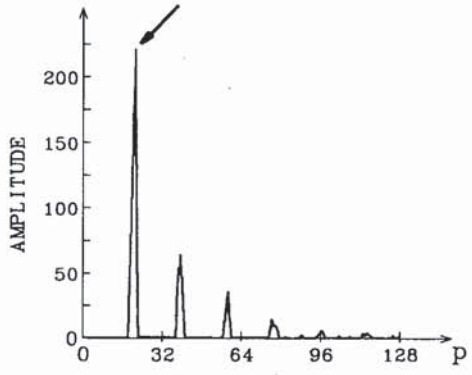

FIG. 13. Negative terms of $C_g(p, 0)$ for the noise-free motion blurred (d = 19) test image (the desired pulse is marked by an arrow).

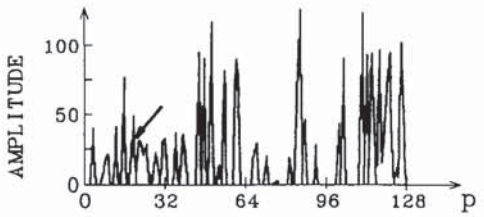

FIG. 14. Negative terms of $C_g(p, 0)$ for the noisy (SNR = 0 dB) and motion blurred (d = 19) test image.

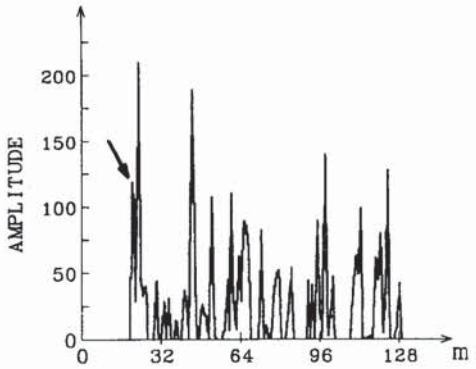

FIG. 15. Negative terms of $C_{\hat{b}}(m)$ for the motion blurred and noisy test image following spectral subtraction.

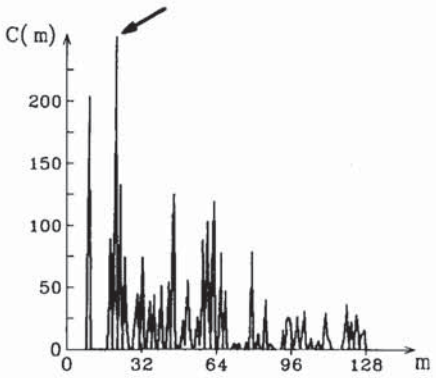

FIG. 16. Cepstral sequence $C(m)$ for the motion blurred and noisy test image obtained by applying the comb lifter to $C_{\hat{b}}(m)$ according to (22).

7. SUMMARY AND CONCLUSIONS

We have presented in this paper an algorithm for identifying the characterizing parameter of the PSF, which corresponds to motion or out-of-focus blur, from noisy blurred images. As in a previously reported work [4], this algorithm is also based on the cepstral domain representation of the image, but is made robust by preprocessing and postprocessing, via spectral subtraction and adaptive

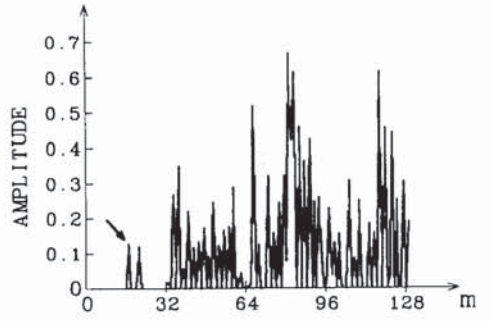

FIG. 17. Negative terms of $C_g(m)$ for the defocused (R = 8) and noisy (SNR = 3 dB) image.

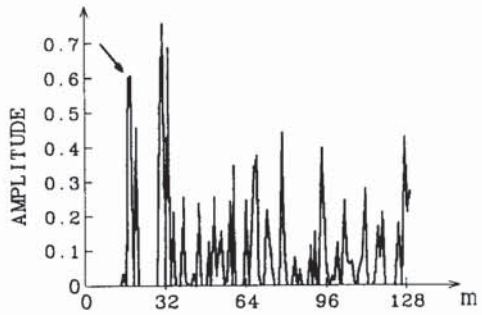

FIG. 18. Negative terms of $C_{\hat{b}}(m)$ for the defocused and noisy test image following spectral subtraction.

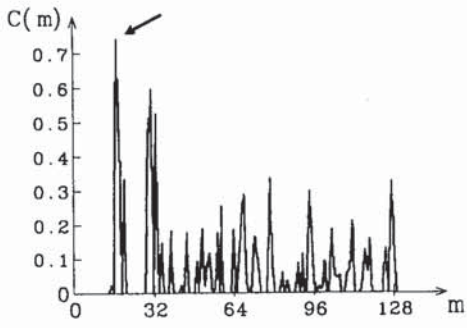

FIG. 19. Cepstral sequence $C(m)$ for out-of-focus blurred and noisy test image obtained at the output of the comb lifter.

comb liftering, respectively. Additional special features are the use of a median-complement filter to estimate the noise; savings in computations from the application of the projection-slice theorem, for motion blur; and circular averaging in the cepstral domain, to combat noise, for out-of-focus blur.

Thus, the proposed algorithm combines processing in the spatial, spectral, and cepstral domains and takes advantage of signal characteristics in each of these domains. It is found to give adequate identification of the blurring function parameter from noisy blurred images with input SNR as low as 0 dB for motion blur and 3 dB for out-of-focus blur. In previous works this was reported only with input SNR of 20 dB and above.

While in most practical applications the input SNR is not as low as 0 or 3 dB, the ability of the algorithm to identify the blur function parameter for such low SNR values proves its robustness to noise. One can therefore apply this algorithm in many applications without being too concerned with how the input SNR would affect the identification of the desired blur parameter.

REFERENCES

1. W. K. Pratt, *Digital Image Processing,* Wiley, New York, 1978.
2. D. B. Gennery, Determination of optical transfer function by inspection of frequency-domain plot, *J. Opt. Soc. Am.* **63**(12), 1973, 1571–1577.
3. T. M. Cannon, *Digital Image Deblurring by Non-Linear Homomorphic Filtering,* Ph.D. dissertation/ARPA. Tech. Rep. UTEC-CSC-74-091, Department of Electrical Engineering, University of Utah, 1974.
4. M. Cannon, Blind deconvolution of spatially invariance image blurs with phase, *IEEE Trans. Acoust. Speech Signal Proces.* **24,** 1976.
5. T. G. Stockham, T. M. Cannon, and R. B. Ingebretsen, Blind deconvolution through digital signal processing, *Proc. IEEE* **63**(4), 1975.
6. E. R. Cole, *The Removal of Unknown Image Blurs by Homomorphic Filtering,* Ph.D. dissertation, Department of Electrical Engineering, University of Utah, 1974.
7. M. Mitre and J. Fleuret, Identification of image degradations, in *Digital Image Processing and Analysis* (J. Simon and A. Rosenfeld, Eds.), Noordhoff, Leyden, The Netherlands, 1977.
8. S. Cooke and T. S. Dorrani, A two-dimensional adaptive image deblurring filter, in *Proceedings, ICASSP-84, San Diego, CA, March 1984,* pp. 37.10.1–37.10A.
9. S. Cooke, A two-dimensional adaptive image deblurring filter, in *Proceedings, IEE Colloquium on Image Restoration and 2-D Filtering Techniques, 1985,* pp. 2/1–6.
10. A. M. Tekalp and H. Kaufman, Maximum likelihood identification of unknown blurs, in *Proceedings, 18th Annual Conference on Information Science and Systems, Princeton, NJ, 1984.*
11. A. M. Tekalp, H. Kaufman, and J. W. Woods, Identification of image and blur parameters for the restoration of noncausal blurs, in *Proceedings, ICASSP-85, Tampa, FL, 1985,* Vol. 2, pp. 656–659.
12. J. Biemond and F. G. Van der Putten, Image restoration using a parallel identification and filtering procedure, in *Proceedings, ICASSP-85, Tampa, FL, 1985,* Vol. 2, pp. 660–663.
13. J. S. Lim, Image restoration by short space spectral subtraction, *IEEE Trans. Acoust. Speech Signal Process.* **28**(2), 1980, 191–197.
14. P. D. Welch, The use of the FFT for the estimation of power spectra, *IEEE Trans. Audio Electroacoust.* **AU-15,** 1967, 70–73.
15. R. W. Schafer *et al.,* Constrained iterative restoration methods, *Proc. IEEE* **69,** 1981, 432–450.
16. A. K. Katsaggelos *et al.,* An iterative method for restoring noisy blurred images, in *Proceedings, ICASSP-84, 1984,* pp. 37.2.1–37.2.4.

17. E. Oja and H. Ogawa, Parametric projection filters for image and signal restoration, *IEEE Trans. Acoust. Speech Signal Process.* **34**(6), 1986, 1643–1653.
18. A. K. Mahalanabis and K. Xue, An efficient two-dimensional Chandrasekhor filter for restoration of images degraded by spatial blur and noise, *IEEE Trans. Acoust. Speech Signal Process.* **35**(11), 1987, 1603–1610.
19. J. Biemond *et al.*, A fast Kalman filter for image degraded by both blur and noise, *IEEE Trans. Acoust. Speech Signal Process.* **31**(5), 1983, 1248–1256.
20. A. Papoulis, *Systems and Transforms with Application to Optics*, McGraw–Hill, New York, 1968.
21. H. C. Andrews and B. R. Hunt, *Digital Image Restoration*, Prentice–Hall, Englewood Cliffs, NJ, 1977.
22. A. Rosenfeld and A. C. Kak, *Digital Picture Processing*, Vol. 2, Academic Press, New York, 1982.
23. R. C. Gonzalez and P. Wintz, *Digital Image Processing*, Addison–Wesley, Reading, MA, 1987.
24. A. K. Jain, *Fundamentals of Digital Image Processing*, Prentice–Hall, Englewood Cliffs, NJ, 1989.
25. J. S. Lim, *Two-Dimensional Signal and Image Processing*, Prentice–Hall, Englewood Cliffs, NJ, 1990.
26. M. I. Sezan and A. M. Teklap, Survey of recent developments in digital image restoration, *Opt. Eng.* **29**(5), 1990, 393–404.
27. A. K. Katsaggelos, Iterative image restoration algorithms, *Opt. Eng.* **28**(7), 1989, 735–748.
28. P. H. Mowforth and Z. P. Jin, Implementation for noise suppression in images, *Opt. Eng.* **28**(7), 1989, 735–748.
29. D. G. Childers *et al.*, The Cepstrum: A guide to processing, *Proc. IEEE* **65**(10), 1977, 1428–1443.